Published in final edited form as:
Hypertension. 2009 June ; 53(6): 1023–1031. doi:10.1161/HYPERTENSIONAHA.108.123422.

Metallothionein Abrogates GTP Cyclohydrolase I inhibition-Induced Cardiac Contractile and Morphological Defect: Role of Mitochondrial Biogenesis

Asli F. Ceylan-Isik[1,*], **Kelly K. Guo**[1,*], **Edward C. Carlson**[2], **Jamie R. Privratsky**[2], **Song-Jie Liao**[3], **Lu Cai**[4], **Alex F. Chen**[3], and **Jun Ren**[1,2]

[1]Center for Cardiovascular Research and Alternative Medicine, University of Wyoming College of Health Sciences, Laramie, WY 82071

[2]University of North Dakota School of Medicine and Health Sciences, Grand Forks, ND 58203

[3]Department of Surgery, University of Pittsburgh School of Medicine, Pittsburgh, PA 15213, and Vascular Surgery Research, Veterans Affairs Pittsburgh Healthcare System, Pittsburgh, PA 15240

[4]Department of Pediatrics, University of Louisville, Louisville, KY 40202

Abstract

One key mechanism for endothelial dysfunction is eNOS uncoupling, whereby eNOS generates $O_2^{\bullet-}$ rather than NO, due to deficient eNOS cofactor tetrahydrobiopterin (BH4). This study was designed to examine the effect of BH4 deficiency on cardiac morphology and function as well as the impact of metallothionein (MT) on BH4 deficiency-induced abnormalities, if any. FVB and cardiac-specific MT transgenic mice were exposed to 2,4-diamino-6-hydroxy-pyrimidine (DAHP, 10 mmol/l, 3 wks), an inhibitor of the BH4 synthetic enzyme GTP cyclohydrolase I. DAHP reduced plasma BH4 levels by 85% and elevated blood pressure in both FVB and MT mice. Echocardiography found decreased fractional shortening and increased end systolic diameter in DAHP-treated FVB mice. Cardiomyocytes from DAHP-treated FVB mice displayed enhanced $O_2^{\bullet-}$ production, contractile and intracellular Ca^{2+} defects including depressed peak shortening and maximal velocity of shortening/relengthening, prolonged duration of relengthening, reduced intracellular Ca^{2+} rise and clearance. DAHP triggered mitochondrial swelling/myocardial filament aberrations and mitochondrial $O_2^{\bullet-}$ accumulation, assessed by TEM and MitoSOX Red fluorescence, respectively. DAHP also promoted the L-NAME inhibitable $O_2^{\bullet-}$ production and eNOS phosphorylation at Thr497. Although MT had little effect on cardiac mechanics and ultrastructure, it attenuated DAHP-induced defects in cardiac function, morphology, $O_2^{\bullet-}$ production and eNOS phosphorylation (Thr497). The DAHP-induced cardiomyocyte mechanical responses were alleviated by *in vitro* BH4 treatment. DAHP inhibited mitochondrial biogenesis, mitochondrial uncoupling protein 2 (UCP2) and chaperone HSP90, all but UCP2 was rescued by MT. Our data suggest a role of BH4 deficiency in cardiac dysfunction and therapeutic potential of antioxidants against eNOS uncoupling in the hearts.

Keywords

BH4; eNOS uncoupling; cardiomyocyte mechanics; metallothionein; superoxide

Corresponding Authors: Dr. Jun Ren Center for Cardiovascular Research and Alternative Medicine, University of Wyoming College of Health Sciences, Laramie, WY 82071, USA Tel: (307)-766-6131; Fax: (307)-766-2953; jren@uwyo.edu.
*These two authors contribute equally to this work.

DISCLOSURES None.

INTRODUCTION

Nitric oxide (NO) is an essential regulator of cardiac contraction although a consensus as to the main cardiac physiological function of NO has only recently emerged by means of genetic deletion or overexpression of all 3 NOS isoforms in cardiomyocytes [1, 2]. Despite their apparent promiscuity, each NOS isozyme appears to correlate with specific signaling events, partially due to their subcellular compartmentation with colocalized effectors and limited NO diffusibility. eNOS is believed to sustain normal cardiac excitation-contraction coupling [3], which is consistent with our data showing that eNOS gene transfer improves cardiomyocyte contractile and intracellular Ca^{2+} properties via a PI-3 kinase-mediated mechanism [4]. An ample amount of experimental evidence has indicated that eNOS can be uncoupled due to enhanced oxidative stress under certain disease states such as hypertension, atherosclerosis and diabetes [5–7]. Functional eNOS oxidizes L-arginine to L-citrulline and NO in the presence of the essential NOS cofactor tetrahydrobiopterin (BH4) [8, 9]. In disease state, BH4 is oxidized by high peroxynitrite ($ONOO^-$) formed by the NO - superoxide ($O_2^{\bullet -}$) reaction, rendering eNOS to produce $O_2^{\bullet -}$ rather than NO in the vasculature (a phenomena known as “eNOS uncoupling”) [9, 10]. Although eNOS uncoupling plays an important role for the pathogenesis of vascular diseases such as endothelial dysfunction and hypertension [10, 11], its impact on the pathophysiology of heart diseases remains poorly understood. We hypothesized that eNOS uncoupling may contribute to the pathogenesis of cardiac dysfunction whereas “eNOS recoupling” through the preserved redox balance is permissive to the maintenance of physiological cardiac function. To this end, the present study was designed to examine the effect of eNOS uncoupling through inhibition of the rate-limiting BH4 synthetic enzyme GTP cyclohydrolase I on murine myocardial contractile function and ultrastructure. Given the prominent role of free radical accumulation and antioxidant reserve in the development of eNOS uncoupling [7, 10], the impact of GTP cyclohydrolase I inhibition was also examined in transgenic mice with overexpression of the thiol-rich metallothionein (MT), a heavy metal scavenger known to preserve the hearts against environmental toxic insults and oxidative damage [12, 13]. 2,4-diamino-6-hydroxy-pyrimidine (DAHP), a selective inhibitor of GTP cyclohydrolase I, was used to block BH4 synthesis [14]. In an effort to elucidate the cellular mechanisms involved in DAHP and MT-induced myocardial alterations, if any, special attention was drawn towards $O_2^{\bullet -}$ production and the peroxisome proliferator-activated receptor γ (PPARγ) coactivator 1α (PGC-1α)-regulated mitochondrial biogenesis. Mitochondrial uncoupling protein 2 (UCP2), a novel member of the mitochondrial anion carrier family, and heat shock protein 90 (HSP90), an essential mitochondrial chaperone, are both involved in the control of mitochondrial function and reactive oxygen species (ROS) generation [15, 16]. Expression of both proteins in association with mitochondrial $O_2^{\bullet -}$ accumulation were evaluated in myocardium from DAHP-treated wild-type Friend Virus B (FVB) and MT transgenic mice.

MATERIALS AND METHODS

See the Methods section in the online supplement for additional details (http://hyper.ahajournals.org).

Experimental animals and DAHP treatment

The experimental protocols have been approved by the Animal Use and Care Committee at the University of Wyoming. Adult male wild-type FVB and cardiac-specific MT overexpression transgenic mice (5 months of age) were fed 2,4-diamino-6-hydroxy-pyrimidine (DAHP, 10 mmol/l) in drinking water for 3 weeks [14]. Since DAHP affects neurotransmitter release such as serotonin and catecholamine which may alter glucose metabolism [17], serum glucose levels were monitored.

Measurement of total biopterin and BH4 levels

Plasma BH4 and total biopterin (BH4, dihydropterin [BH2] and oxidized biopterin [B]) levels were measured by HPLC with florescence detection as described [18].

Echocardiographic assessment

Cardiac geometry and function were evaluated using a 2-D guided M-mode echocardiography equipped with a 15-6 MHz linear transducer. Fractional shortening was calculated from end-diastolic diameter (EDD) and end-systolic diameter (ESD) using the equation of (EDD-ESD)/EDD [19].

Intracellular fluorescence measurement of $O_2^{\bullet-}$

Myocytes loaded with dihydroethidium (DHE, 5 μmol/l) were sampled using an Olympus BX-51 microscope equipped with an Olympus MagnaFire™ SP digital camera and an ImagePro image analysis software [20].

HPLC fluorescence detection of $O_2^{\bullet-}$

2-hydroxyethidium (2-OH-E^+), a product formed from the reaction of $O_2^{\bullet-}$ and hydroethidine (HE), is considered a more suitable probe for intracellular $O_2^{\bullet-}$ 21. HE, ethidium (E^+) and 2-OH-E^+ were separated by an HPLC system equipped with a fluorescence detector [21].

MitoSOX Red fluorescence measurement of mitochondrial $O_2^{\bullet-}$

Cells loaded with MitoSOX Red (2 μmol/l) were rinsed and MitoSOX Red fluorescence intensity was captured at 510/580 nm using an Olympus BX51 microscope equipped with a digital cooled charged-coupled device camera [22].

Cardiomyocyte isolation and mechanics

Mouse cardiomyocytes were isolated as described [12]. Mechanical properties of myocytes were assessed using an IonOptix™ soft-edge system [12]. Cell shortening and relengthening were assessed using the following indices: peak shortening (PS), time-to-PS (TPS), time-to-90% relengthening (TR_{90}) and maximal velocities of shortening/relengthening (± dL/dt).

Intracellular Ca^{2+} transients and sacroplasmic reticulum (SR) Ca^{2+} release

Myocytes loaded with fura-2/AM (0.5 μmol/l) were exposed to lights emitted through either a 360 or a 380 nm filter. Fluorescence emissions were detected between 480–520 nm [12]. SR Ca^{2+} release was assessed by rapid puff of caffeine (10 mmol/l)-induced intracellular Ca^{2+} transients in fura-2-loaded myocytes [23].

Electron microscopy

Following perfusion fixation, left ventricular and interventricular septal tissues were minced to 1 mm^3 followed by fixation and postfixation. Tissue blocks were embedded in Epon/Araldite and cured 48 hr at 60°C. Thin sections were collected on naked copper (300-mesh) grids, stained with lead citrate and uranyl acetate, and imaged with a Hitachi 7500 transmission electron microscope [19].

Western blot analysis

Membrane proteins were separated on SDS-polyacrylamide gels and were transferred to polyvinylidene difluoride membranes. The membranes were blocked with 5% milk and then incubated overnight with specific antibodies. The antigens were detected by the luminescence method [19].

Total RNA extraction, cDNA synthesis, reverse transcription and real-time PCR

Total RNA extraction, cDNA synthesis and real-time PCR were carried out as described [12].

Data analysis

Mean ± SEM. Statistical significance ($p < 0.05$) was estimated by ANOVA followed by a Tukey's test for *post hoc* analysis where appropriate.

RESULTS

General morphometric and echocardiographic characteristics

As shown in Table 1, DAHP and MT transgene failed to elicit any effects on body, heart, liver or kidney weights, organ size (normalized to body weight), heart rate, EDD, LV mass (absolute and normalized) and blood glucose. DAHP moderately but significantly elevated both systolic and diastolic blood pressure, the effect of which was unaffected by MT. DAHP treatment significantly increased ESD but reduced wall thickness and fractional shortening, which were significantly attenuated by MT transgene. MT itself did not affect myocardial geometry and fractional shortening. As expected, blockade of GTP cyclohydrolase I with DAHP significantly reduced total biopterin (by 64%) and BH4 (by 85%) levels regardless of MT overexpression or not. Measurement of $O_2^{\bullet -}$ levels using DHE fluorescence revealed enhanced $O_2^{\bullet -}$ levels in cardiomyocytes from DAHP-treated FVB but not MT mice. DAHP-elicited increased of $O_2^{\bullet -}$ production was significantly attenuated by the NOS inhibitor L-NAME (100 μmol/l), indicating the presence of eNOS uncoupling (Fig. 1A–1C). Furthermore, DAHP promoted eNOS phosphorylation at the Thr497 residue without any effect on total eNOS expression, which is another hallmark of eNOS uncoupling [9]. Consistent with its effect on the DAHP-induced $O_2^{\bullet -}$ production, MT nullified the DAHP-elicited phosphorylation of eNOS at Thr497 (Fig. 1D). Given that oxidation of HE to 2-OH-E^+ was used as a more suitable measurement to quantify the production of $O_2{}^{*-}$21, HPLC fluorescence detection was performed for 2-OH-E^+ levels Our data revealed that DAHP stimulated the SOD-inhibitable $O_2^{\bullet -}$ production in FVB but not MT mice. Our result also indicated that MT transgene did not have any effect on 2-OH-E^+ production (Fig. 2).

Effect of DAHP and BH4 on cardiomyocyte mechanical and fluorescent properties

DAHP treatment had no overt effect on cell phenotype (data not shown). The resting cell length (CL) of cardiomyocytes was comparable between FVB and MT groups, regardless of DAHP treatment. Cardiomyocytes from the FVB-DAHP group exhibited significantly depressed PS, reduced ± dL/dt and prolonged TR_{90} associated with comparable TPS. Interestingly, cardiac overexpression of MT abrogated the DAHP-induced changes in PS, ± dL/dt and TR_{90} without eliciting any significant effect by itself. To further examine the role of BH4 deficiency in these mechanical aberrations, cardiomyocytes from DAHP-treated FVB mice were incubated *in vitro* with BH4 (10 μmol/l) for 4 hrs prior to mechanical assessment. Our results depicted that BH4 significantly alleviated the DAHP-induced cardiomyocyte mechanical dysfunction in a manner reminiscent of MT transgene (Fig. 3). To explore the mechanism of action behind DAHP, MT and BH4-induced mechanical responsiveness, intracellular Ca^{2+} transients were recorded using fura-2 fluorescence in cardiomyocytes from FVB and MT mice with or without DAHP treatment. Fig. 4 displays that DAHP depressed the electrically-stimulated rise in fura-2 fluorescent intensity (ΔFFI), SR Ca^{2+} release and prolonged intracellular Ca^{2+} decay without affecting baseline intracellular Ca^{2+} FFI. While MT itself did not affect any of these intracellular Ca^{2+} properties, it prevented the DAHP-induced depression in ΔFFI, SR Ca^{2+} release and intracellular Ca^{2+} clearance. Consistent with the mechanical data, *in vitro* BH4 incubation significantly attenuated the DAHP-induced dysregulation in intracellular Ca^{2+} homeostasis.

Electron microscopy in myocardium from FVB and MT mice following DAHP treatment

Without DAHP treatment, little ultrastructural difference was noticeable in myocardial samples between FVB and MT groups. DAHP treatment triggered extensive focal damage in left ventricular and intraventricular septal (data not shown) myocardial tissue sections in FVB group. This was evidenced by cytoarchitectural damage including mitochondrial swelling and overtly disrupted sarcomeres and myofilament array. Consistent with the mechanical observations, MT alleviated the DAHP-induced cardiac unltrastructural damage (Fig. 5). Myocardial tissues from MT-DAHP mice were ultrastructurally indistinguishable from control samples.

Mitochondrial biogenesis: PGC-1α, its downstream factors and mtDNA copy number

Given the above ultrastructural finding of mitochondrial anomalies in response to DAHP treatment and the proven association between eNOS uncoupling and mitochondrial damage in endothelial cells [24], the impact of DAHP and MT on the expression of the mitochondrial biogenesis regulator PGC-1α and its downstream factors including nuclear respiratory factor 1, 2 (NRF1, NRF2), mitochondrial transcription factor A (mtTFA) as well as mtDNA copy number [25] was examined. Our data revealed that DAHP significantly down-regulated PGC-1α by ~20% associated with marked reductions in mRNA levels of NRF1, NRF2 and mtTFA. MT effectively alleviated the DAHP-induced depression of PGC-1α and its downstream nuclear factors with little effect by itself. The mtDNA copy number, a key index for oxidative mitochondrial damage and mitochondrial biogenesis, was also downregulated following DAHP treatment, the effect of which was reversed by MT (Fig. 6, S1).

Western blot analysis for UCP2, HSP90 and mitochondrial $O_2^{\bullet-}$ production

Immunoblot analysis exhibited that DAHP treatment significantly reduced expression of mitochondrial uncoupling protein UCP2 and mitochondrial chaperone HSP90, both of which are closely associated with mitochondrial dysfunction, oxidative stress and heart failure [15, 16]. Although MT transgene itself did not alter protein expression of UCP2 and HSP90, it attenuated the DAHP-induced decline in protein expression of HSP90 but not UCP2 (see online supplement Fig. S1). To further evaluate mitochondrial damage and its potential contribution to the enhanced intracellular $O_2^{\bullet-}$ generation, mitochondrial $O_2^{\bullet-}$ production was detected using the MitoSOX Red probe. DAHP significantly promoted mitochondrial $O_2^{\bullet-}$ production in cardiomyocytes from FVB but not MT mice. MT itself did not elicit any significant effect on mitochondrial $O_2^{\bullet-}$ production (see online supplement Fig. S2).

DISCUSSION

The major findings of our study are that BH4 deficiency with DAHP treatment directly leads to moderate elevation in blood pressure, cardiac contractile dysfunction, intracellular Ca^{2+} dysregulation, deranged myocardial ultrastructure, loss of mitochondrial biogenesis, reduced expression of UCP2 and HSP90, as well as enhanced intracellular/mitochondrial $O_2^{\bullet-}$ levels and theronine 497 phosphorylation of eNOS, all of which with the exception of elevated blood pressure and downregulated UCP2 were alleviated by the free radical scavenger MT. Our study demonstrated for the first time myocardial contractile and intracellular Ca^{2+} dysfunctions associated with morphological aberration associated with BH4 deficiency and eNOS uncoupling. The deranged cardiac ultrastructural integrity including mitochondrial swelling and anomalies in contractile filament further confirmed that the myopathy is focal to cardiomyocytes and mitochondria. Our observation that MT abrogates the DAHP-induced changes in cardiac mechanical function and ultrastructural integrity indicates the therapeutic potential of antioxidants in eNOS uncoupling-induced cardiac injury.

Inhibition of GTP cyclohydrolase I is considered a rather selective tool to assess the role of *de novo* synthesis of BH4 in a given biological system [14, 17]. To this end, DAHP has been widely used as the prototypical GTP cyclohydrolase I inhibitor [14, 17, 26]. Our present study revealed that specific GTP cyclohydrolase I inhibition leads to elevated blood pressure which is not affected by cardiac overexpression of MT, thus not favoring a role of blood pressure regulation in the DAHP and MT-induced responses on myocardial function and ultrastructure. DAHP markedly reduced levels of both total biopterin and BH4, depressed peak shortening, depressed maximal velocities of shortening/relengthening, prolonged relengthening duration and intracellular Ca^{2+} clearance as well as reduced intracellular Ca^{2+} recruitment and SR Ca^{2+} release capacity. These observations indicated the presence of compromised cardiac contractile function, consistent with our previous report of cardiac excitation-contraction dysfunction under oxidant injury [19]. The deleterious effects of DAHP may be explained by increased $O_2^{\bullet-}$ due to the uncoupled eNOS. BH4 depletion is known to prompt eNOS to produce $O_2^{\bullet-}$ instead of NO as a result of the theronine 497 rather than serine 1179 phosphorylation of eNOS [9], consistent with our finding of enhanced Thr497 phosphorylation. Our observation that L-NAME is capable of inhibiting the DAHP-elicited $O_2^{\bullet-}$ production further consolidated the presence of eNOS uncoupling in our current experimental setting. $O_2^{\bullet-}$ accumulation has been demonstrated to result in myocardial contractile dysfunction, rigor and cytosolic Ca^{2+} overload [27, 28]. In addition, $O_2^{\bullet-}$ and other free radicals may disrupt intracellular Ca^{2+} homeostasis through inhibition of L-type Ca^{2+} currents, SR Ca^{2+} load, Na^{+}-Ca^{2+} exchange and SR Ca^{2+} uptake 27, 28, *en route* to compromised cardiac contractility, contraction and relaxation duration consistent with the reduced fractional shortening, PS, ± dL/dt, prolonged TR_{90} and intracellular Ca^{2+} decay found in our study. TPS and resting intracellular Ca^{2+} were spared by DAHP treatment, indicating possible disparity in the sensitivity of cardiac contractile/Ca^{2+} regulating proteins to myocardial eNOS uncoupling. Prolonged duration of contraction and relaxation, delayed intracellular Ca^{2+} clearance and dampened intracellular Ca^{2+} release are considered hallmarks of cardiomyopathy in a number of disease states such as heart failure, hypertension, obesity, diabetes and oxidative stress [12, 13, 19, 23, 28, 29]. The alterations in mechanical and intracellular Ca^{2+} properties observed in our study, although relatively small (~20%), were consistent with the degree change from failing human hearts [29], and were further supported by the apparent cardiac remodeling (changes in wall thickness and ESD) and focal structural damage (mitochondrial swelling and displacement of cardiac contractile filaments) following chronic DAHP treatment. Mitochondria, a main target for $O_2{}^{*-}$, exhibit mitochondrial permeability transition leading to mitochondrial swelling, cytochrome *c* release, loss of biogenesis and function in response to sustained $O^{\bullet-}$ challenge [24]. This is consolidated by our data of lost mitochondrial biogenesis, UCP2 and HSP90 as well as mitochondrial $O_2^{\bullet-}$ generation following DAHP treatment. Collectively, our data favored an essential role of BH4 and functional eNOS in the maintenance of cardiac functional and ultrastructural integrity under physiological conditions.

Perhaps the most interesting finding of our study is that cardiac-specific overexpression of MT prevents cardiac functional, ultrastructural, $O_2^{\bullet-}$ production, and protein disarray associated with DAHP treatment. MT failed to elicit any effect on the loss of total biopterin and BH4 although it mimicked BH4 supplementation-elicited protection against DAHP-induced detrimental effects on cardiomyocyte mechanical and intracellular Ca^{2+} properties. Given that MT alleviated DAHP-induced L-NAME-inhibitable intracellular $O_2^{\bullet-}$ production and theronine 497 phosphorylation of eNOS, it is plausible to speculate that the MT transgene may protect against DAHP-induced cardiac injury through counteracting “eNOS uncoupling”. Despite the low plasma BH4 levels, MT may efficiently scavenge the $O_2^{\bullet-}$ and other free radicals in cardiomyocytes thus prompting the “eNOS recoupling”. Administration of antioxidants such as L-ascorbic acid or the eNOS coupler folic acid has been shown to improve endothelial function through “eNOS dimerization or eNOS recoupling” [10, 30, 31]. Furthermore, our data revealed that MT abrogated the DAHP-induced mitochondrial damage, mitochondrial

$O_2^{\bullet-}$ production, loss of mitochondrial DNA, and downregulation of mitochondrial biogenesis factor PGC-1α and its downstream nuclear factors. Reduced mitochondrial biogenesis and downregulation of genes required for mitochondrial oxidative phosphorylation have been implicated in insulin resistance and type 2 diabetes [12, 32]. PGC-1α promotes mitochondrial genes by enhancing levels of NRF1 and NRF2, alternatively called GA-binding protein (GABP), and facilitate GABP binding to regulatory regions of mtTFA promoter [25]. It is reasonable to speculate that eNOS uncoupling-induced downregulation of PGC-1α, NRF1, NRF2 and mtTFA contributes to the loss of mitochondrial DNA and biogenesis. PGC-1α is crucial for normal heart function as PGC-1α knockout or deficiency results in compromised cardiac function [25]. The precise mechanism responsible for loss of mitochondrial biogenesis under eNOS uncoupling is unknown although certain posttranslational oxidative modification may play a role [25]. Our findings demonstrated the ability of MT to compensate for the DAHP-induced downregulation of HSP90. Reduction of the mitochondrial chaperon HSP90 has been implicated as an event secondary to uncoupling of eNOS, leading to mitochondrial dysfunction and dysregulated endothelial function associated with cardiovascular diseases [16]. Our results suggest that the antioxidant protection against downregulated HSP90 but not mitochondrial UCP2 may contribute to the beneficial effect of MT on mitochondrial integrity. Last but not the least, nNOS and iNOS are constitutively expressed or pathologically induced, respectively, in cardiomyocytes. Both NOS isoforms participate in the modulation of myocardial functions including inotropy, relaxation, β-adrenergic responsiveness, and force-frequency relationship [33]. Further study is warranted to elucidate the role other NOS isoforms in the antioxidant-offered beneficial effects in myocardial function in the state of eNOS uncoupling.

PERSPECTIVES

Our present work has provided evidence that eNOS uncoupling directly triggers cardiac ultrastructural and functional anomalies associated with mitochondrial oxidative and biogenesis damage. These results have consolidated a role of functional eNOS in the maintenance of cardiac physiology and more importantly, the therapeutic value of antioxidants against the eNOS uncoupling-induced cardiac pathology. Our data also indicated the therapeutic value of BH4 and GTP cyclohydrolase I in the management of cardiovascular dysfunction [10, 34]. Furthermore, it prompts the speculation that eNOS uncoupling seen in the clinical conditions of vascular injuries such as hypertension and atherosclerosis may account, at least in part, for the increased cardiac events under these conditions. Therefore, eNOS recoupling may benefit both vascular anomalies and cardiac pathologies.

Acknowledgments

The authors greatly appreciated the technical assistance of Dr. Kurt Dolence and Bonnie Zhao from University of Wyoming College of Health Sciences as well as Donna Laturnus and Janice Audette from the University of North Dakota Department of Anatomy and Cell Biology. MT transgenic line was kindly provided by Dr. Paul N. Epstein from University of Louisville.

SOURCE OF FUNDING This work was supported in part by grants from the American Diabetes Association (7-08-RA-130), the American Heart Association Pacific Mountain Affiliate (#0355521Z), the NIH/NCRR University of Wyoming North Rockies Regional INBRE (P20 RR016474) to JR; American Diabetes Association (7-05-CD-02) to LC; NIH R01 GM077352, American Diabetes Association (7-08-RA-23), the American Heart Association (0855601G) to AFC. SJL was an awardee of the AHA Postdoctoral Fellowship 0720118Z.

Reference List

(1). Belge C, Massion PB, Pelat M, Balligand JL. Nitric oxide and the heart: update on new paradigms. Ann N Y Acad Sci 2005;1047:173–182. [PubMed: 16093495]

(2). Massion PB, Balligand JL. Modulation of cardiac contraction, relaxation and rate by the endothelial nitric oxide synthase (eNOS): lessons from genetically modified mice. J Physiol 2003;546:63–75. [PubMed: 12509479]

(3). Massion PB, Pelat M, Belge C, Balligand JL. Regulation of the mammalian heart function by nitric oxide. Comp Biochem Physiol A Mol Integr Physiol 2005;142:144–150. [PubMed: 15985381]

(4). Ren J, Zhang X, Scott GI, Esberg LB, Ren BH, Culver B, Chen AF. Adenovirus gene transfer of recombinant endothelial nitric oxide synthase enhances contractile function in ventricular myocytes. J Cardiovasc Pharmacol 2004;43:171–177. [PubMed: 14716202]

(5). Oak JH, Cai H. Attenuation of Angiotensin II Signaling Recouples eNOS and Inhibits Nonendothelial NOX Activity in Diabetic Mice. Diabetes 2007;56:118–126. [PubMed: 17192473]

(6). Hink U, Li H, Mollnau H, Oelze M, Matheis E, Hartmann M, Skatchkov M, Thaiss F, Stahl RA, Warnholtz A, Meinertz T, Griendling K, Harrison DG, Forstermann U, Munzel T. Mechanisms underlying endothelial dysfunction in diabetes mellitus. Circ Res 2001;88:E14–E22. [PubMed: 11157681]

(7). Alp NJ, McAteer MA, Khoo J, Choudhury RP, Channon KM. Increased endothelial tetrahydrobiopterin synthesis by targeted transgenic GTP-cyclohydrolase I overexpression reduces endothelial dysfunction and atherosclerosis in ApoE-knockout mice. Arterioscler Thromb Vasc Biol 2004;24:445–450. [PubMed: 14707037]

(8). Antoniades C, Shirodaria C, Warrick N, Cai S, de Bono J, Lee J, Leeson P, Neubauer S, Ratnatunga C, Pillai R, Refsum H, Channon KM. 5-methyltetrahydrofolate rapidly improves endothelial function and decreases superoxide production in human vessels: effects on vascular tetrahydrobiopterin availability and endothelial nitric oxide synthase coupling. Circulation 2006;114:1193–1201. [PubMed: 16940192]

(9). Lin MI, Fulton D, Babbitt R, Fleming I, Busse R, Pritchard KA Jr. Sessa WC. Phosphorylation of threonine 497 in endothelial nitric-oxide synthase coordinates the coupling of L-arginine metabolism to efficient nitric oxide production. J Biol Chem 2003;278:44719–44726. [PubMed: 12952971]

(10). Forstermann U, Munzel T. Endothelial nitric oxide synthase in vascular disease: from marvel to menace. Circulation 2006;113:1708–1714. [PubMed: 16585403]

(11). Schulz E, Jansen T, Wenzel P, Daiber A, Munzel T. Nitric oxide, tetrahydrobiopterin, oxidative stress, and endothelial dysfunction in hypertension. Antioxid Redox Signal 2008;10:1115–1126. [PubMed: 18321209]

(12). Dong F, Li Q, Sreejayan N, Nunn JM, Ren J. Metallothionein prevents high-fat diet induced cardiac contractile dysfunction: role of peroxisome proliferator activated receptor gamma coactivator 1alpha and mitochondrial biogenesis. Diabetes 2007;56:2201–2212. [PubMed: 17575086]

(13). Ye G, Metreveli NS, Ren J, Epstein PN. Metallothionein prevents diabetes-induced deficits in cardiomyocytes by inhibiting reactive oxygen species production. Diabetes 2003;52:777–783. [PubMed: 12606520]

(14). Mitchell BM, Dorrance AM, Webb RC. Phenylalanine improves dilation and blood pressure in GTP cyclohydrolase inhibition-induced hypertensive rats. J Cardiovasc Pharmacol 2004;43:758–763. [PubMed: 15167268]

(15). Lee KU, Lee IK, Han J, Song DK, Kim YM, Song HS, Kim HS, Lee WJ, Koh EH, Song KH, Han SM, Kim MS, Park IS, Park JY. Effects of recombinant adenovirus-mediated uncoupling protein 2 overexpression on endothelial function and apoptosis. Circ Res 2005;96:1200–1207. [PubMed: 15905464]

(16). Sud N, Wells SM, Sharma S, Wiseman DA, Wilham J, Black SM. Asymmetric dimethylarginine inhibits HSP90 activity in pulmonary arterial endothelial cells: role of mitochondrial dysfunction. Am J Physiol Cell Physiol 2008;294:C1407–C1418. [PubMed: 18385287]

(17). Kobayashi T, Hasegawa H, Kaneko E, Ichiyama A. Gastrointestinal serotonin: depletion due to tetrahydrobiopterin deficiency induced by 2,4-diamino-6-hydroxypyrimidine administration. J Pharmacol Exp Ther 1991;256:773–779. [PubMed: 1825228]

(18). Zheng JS, Yang XQ, Lookingland KJ, Fink GD, Hesslinger C, Kapatos G, Kovesdi I, Chen AF. Gene transfer of human guanosine 5'-triphosphate cyclohydrolase I restores vascular

tetrahydrobiopterin level and endothelial function in low renin hypertension. Circulation 2003;108:1238–1245. [PubMed: 12925450]

(19). Ren J, Privratsky JR, Yang X, Dong F, Carlson EC. Metallothionein alleviates glutathione depletion-induced oxidative cardiomyopathy in murine hearts. Crit Care Med 2008;36:2106–2116. [PubMed: 18552690]

(20). Dong F, Zhang X, Ren J. Leptin regulates cardiomyocyte contractile function through endothelin-1 receptor-NADPH oxidase pathway. Hypertension 2006;47:222–229. [PubMed: 16380530]

(21). Zhao H, Joseph J, Fales HM, Sokoloski EA, Levine RL, Vasquez-Vivar J, Kalyanaraman B. Detection and characterization of the product of hydroethidine and intracellular superoxide by HPLC and limitations of fluorescence. Proc Natl Acad Sci USA 2005;102:5727–5732. [PubMed: 15824309]

(22). Song Y, Du Y, Prabhu SD, Epstein PN. Diabetic Cardiomyopathy in OVE26 Mice Shows Mitochondrial ROS Production and Divergence Between In Vivo and In Vitro Contractility. Rev Diabet Stud 2007;4:159–168. [PubMed: 18084673]

(23). Relling DP, Esberg LB, Fang CX, Johnson WT, Murphy EJ, Carlson EC, Saari JT, Ren J. High-fat diet-induced juvenile obesity leads to cardiomyocyte dysfunction and upregulation of Foxo3a transcription factor independent of lipotoxicity and apoptosis. J Hypertens 2006;24:549–561. [PubMed: 16467659]

(24). Munzel T, Sinning C, Post F, Warnholtz A, Schulz E. Pathophysiology, diagnosis and prognostic implications of endothelial dysfunction. Ann Med 2008;40:180–196. [PubMed: 18382884]

(25). Handschin C, Spiegelman BM. The role of exercise and PGC1alpha in inflammation and chronic disease. Nature 2008;454:463–469. [PubMed: 18650917]

(26). Kolinsky MA, Gross SS. The mechanism of potent GTP cyclohydrolase I inhibition by 2,4-diamino-6-hydroxypyrimidine: requirement of the GTP cyclohydrolase I feedback regulatory protein. J Biol Chem 2004;279:40677–40682. [PubMed: 15292175]

(27). Esberg LB, Ren J. The oxygen radical generator pyrogallol impairs cardiomyocyte contractile function via a superoxide and p38 MAP kinase-dependent pathway: protection by anisodamine and tetramethylpyrazine. Cardiovasc Toxicol 2004;4:375–384. [PubMed: 15531780]

(28). Goldhaber JI, Qayyum MS. Oxygen free radicals and excitation-contraction coupling. Antioxid Redox Signal 2000;2:55–64. [PubMed: 11232601]

(29). von LD, Bruns S, Walther S, Kogler H, Pieske B. Insulin causes [Ca2+]i-dependent and [Ca2+]i-independent positive inotropic effects in failing human myocardium. Circulation 2005;111:2588–2595. [PubMed: 15883206]

(30). Forstermann U. Janus-faced role of endothelial NO synthase in vascular disease: uncoupling of oxygen reduction from NO synthesis and its pharmacological reversal. Biol Chem 2006;387:1521–1533. [PubMed: 17132097]

(31). Moat SJ, Clarke ZL, Madhavan AK, Lewis MJ, Lang D. Folic acid reverses endothelial dysfunction induced by inhibition of tetrahydrobiopterin biosynthesis. Eur J Pharmacol 2006;530:250–258. [PubMed: 16387296]

(32). Boirie Y. Insulin regulation of mitochondrial proteins and oxidative phosphorylation in human muscle. Trends Endocrinol Metab 2003;14:393–394. [PubMed: 14580754]

(33). Seddon M, Shah AM, Casadei B. Cardiomyocytes as effectors of nitric oxide signalling. Cardiovasc Res 2007;75:315–26. [PubMed: 17568574]

(34). Du YH, Guan YY, Alp NJ, Channon KM, Chen AF. Endothelium-specific GTP cyclohydrolase I overexpression attenuates blood pressure progression in salt-sensitive low-renin hypertension. Circulation 2008;117:1045–1054. [PubMed: 18268143]

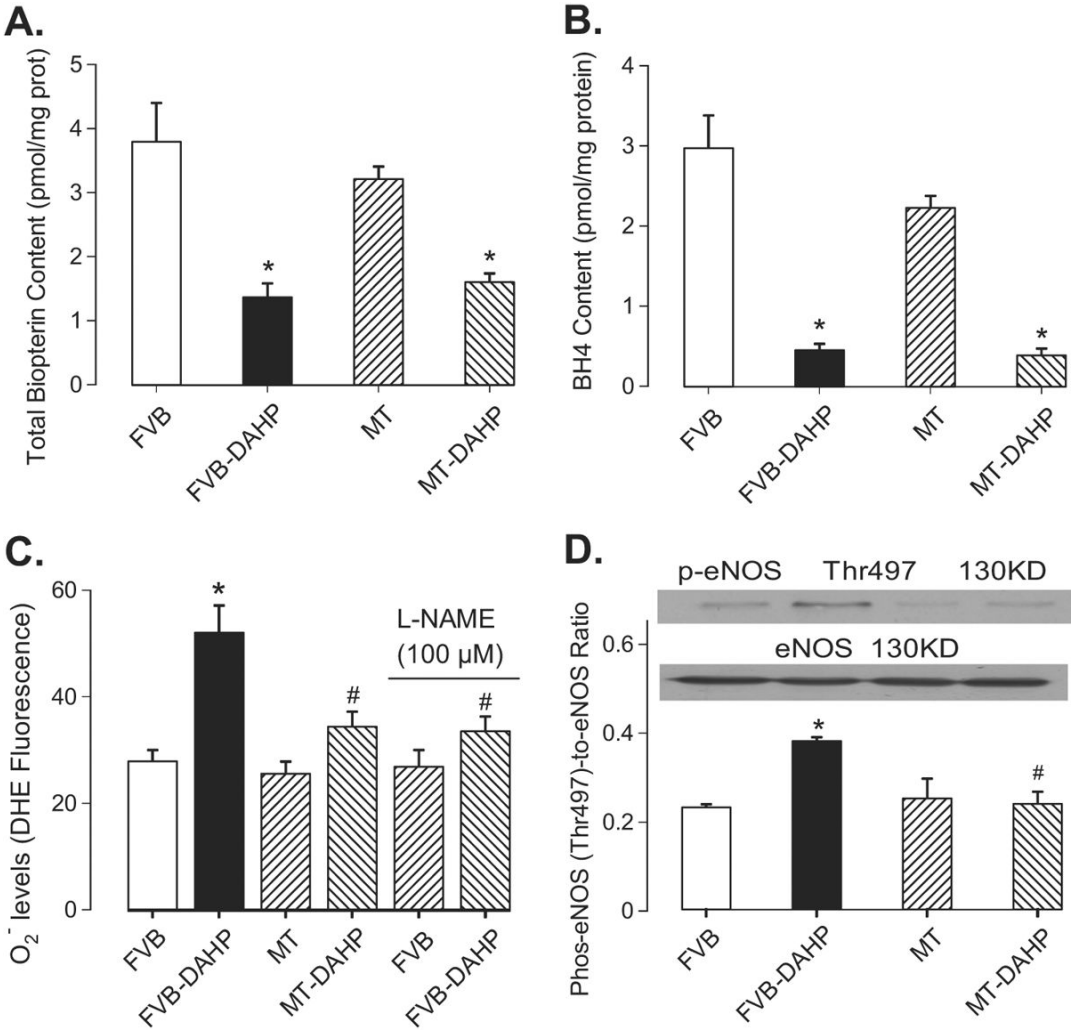

Fig. 1.

Effect of DAHP on content of total biopterin (panel A), BH4 (panel B), O_2*– levels in the absence or presence of the NOS inhibitor L-NAME (100 μmol/l) (panel C) and p-eNOS (Thr497) (panel D) in FVB and MT mice. Inset: Representative gel blots of p-eNOS and total eNOS. Mean ± SEM, n = 5–7, * $p<0.05$ *vs*. FVB, # $p<0.05$ *vs*. FVB-DAHP group.

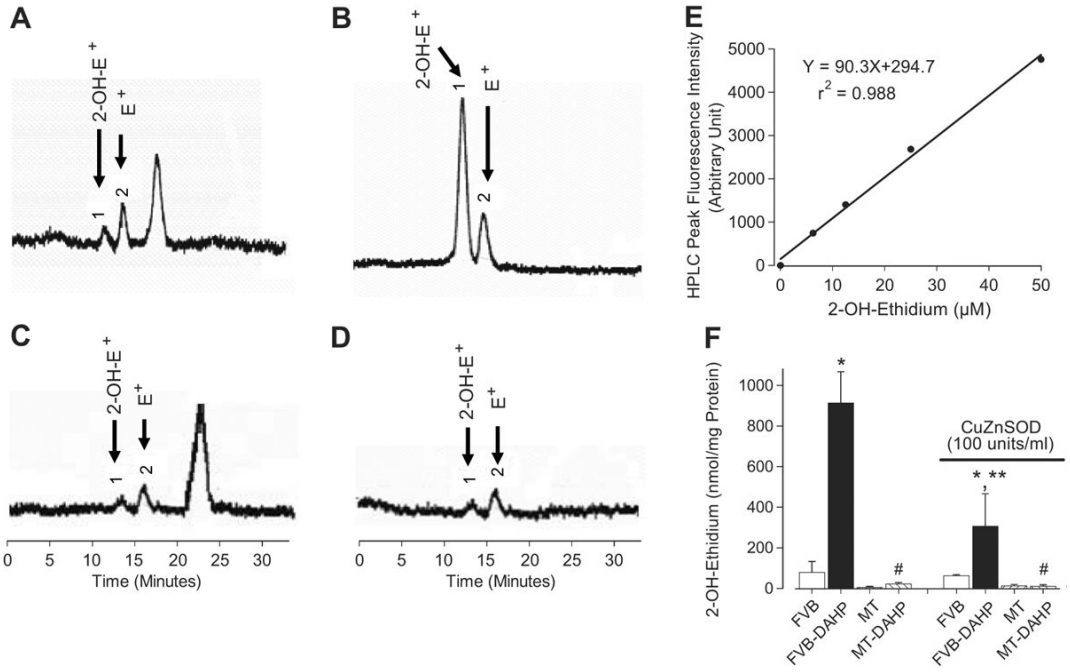

Fig. 2.

HPLC identification of 2-OH-E^+ from the $O_2^{\bullet}$–/HE reaction in cardiomyocytes. Panels A – D display the HPLC chromatograms from FVB (A), FVB-DAHP (B), MT (C) and MT-DAHP (D) groups. Panel E: Standard HPLC peak intensity of authentic 2-OH-E^+. Panel F: Levels of 2-OH-E^+ in FVB, FVB-DAHP, MT and MT-DAHP groups with or without copper zinc SOD (100 units/ml). 2-OH-E^+: 2-Hydroxyethidium (labeled peak 1); E^+: Ethidium (labeled peak 2). Mean ± SEM, n = 100–120 cells per group, * $p<0.05$ *vs*. FVB, # $p<0.05$ *vs*. respective FVB-DAHP group, ** $p<0.05$ *vs*. FVB-DAHP group in the absence of SOD.

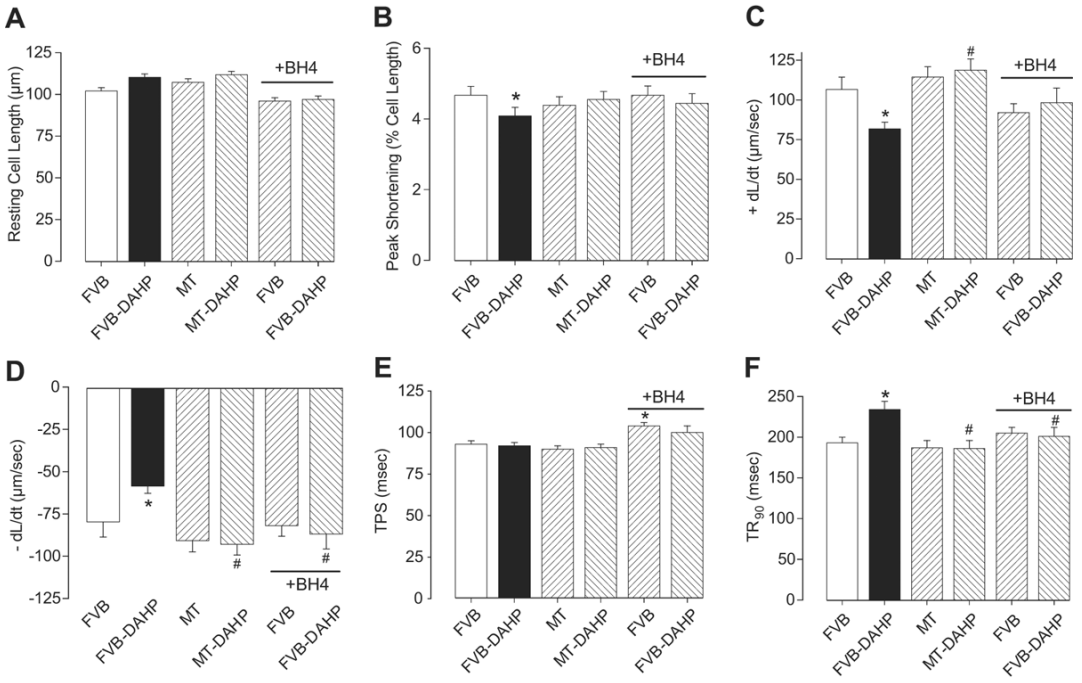

Fig. 3.

Effect of DAHP-induced response on cardiomyocyte contractile function in FVB and MT mice. A cohort of cardiomyocytes from FVB and FVB-DAHP groups was incubated with BH4 (10 µmol/l) for 4 hrs prior to mechanical assessment. (A): Resting cell length; (B): Peak cell shortening; (C): + dL/dt; (D): − dL/dt; (E): TPS; and (F): TR_{90}. Mean ± SEM, n = 132–133 cells from 6 mice per group, * $p<0.05$ *vs*. FVB, # $p<0.05$ *vs*. FVB-DAHP.

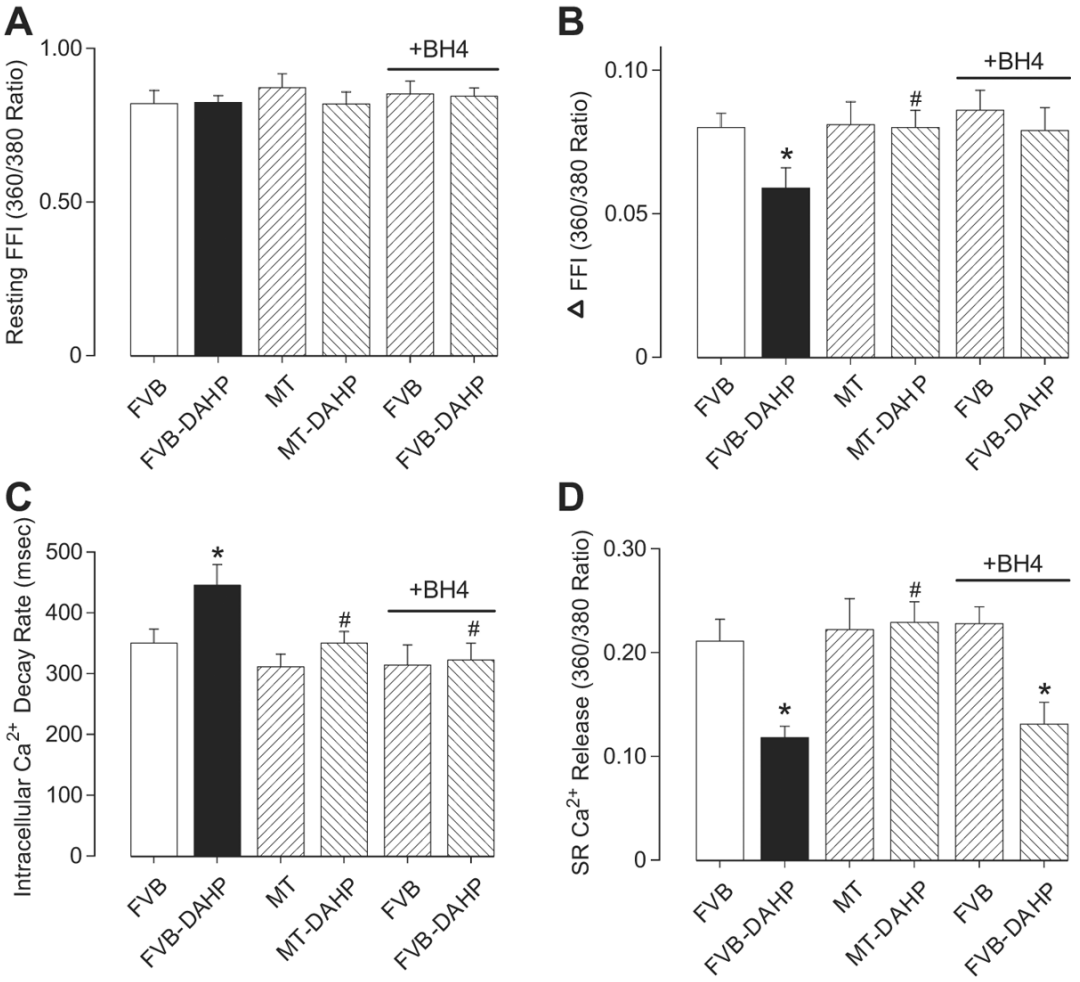

Fig. 4.

Effect of DAHP on intracellular Ca2+ transients and SR Ca^{2+} release in cardiomyocytes from FVB and MT mice. A cohort of cardiomyocytes from FVB and FVB-DAHP groups was incubated with BH4 (10 μmol/l) for 4 hrs prior to intracellular Ca^{2+} assessment. (A): Baseline intracellular Ca^{2+} fura-2 fluorescent intensity (FFI); (B): Change of fura-2 fluorescence intensity in response to electrical stimulation (ΔFFI); (C): Intracellular Ca^{2+} fluorescence decay rate; and (D): SR Ca^{2+} release. Mean ± SEM, n = 68–70 cells (7 cells for SR Ca^{2+} release) per group, * $p<0.05$ *vs*. FVB; # $p<0.05$ *vs*. FVB-DAHP.

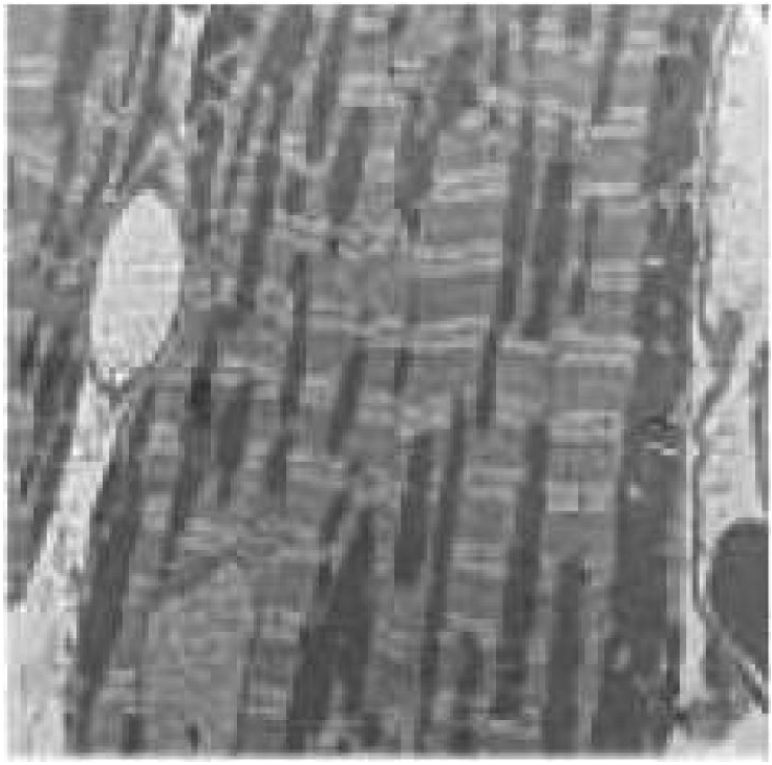

Fig. 5.

Transmission electron microscopic micrographs of left ventricular heart tissues from FVB and MT mice with or without DAHP treatment. (A): FVB; (B): FVB-DAHP; (C): MT; and (D): MT-DAHP. Myocardial tissues in A, C and D appear normal with myofibrils composed of regular and uninterrupted sarcomeres separated by continuous rows of normal mitochondria. In the myocardium from FVB-DAHP mice, irregularly shaped mitochondria and myelin figures are randomly distributed between highly disrupted myofibrils.

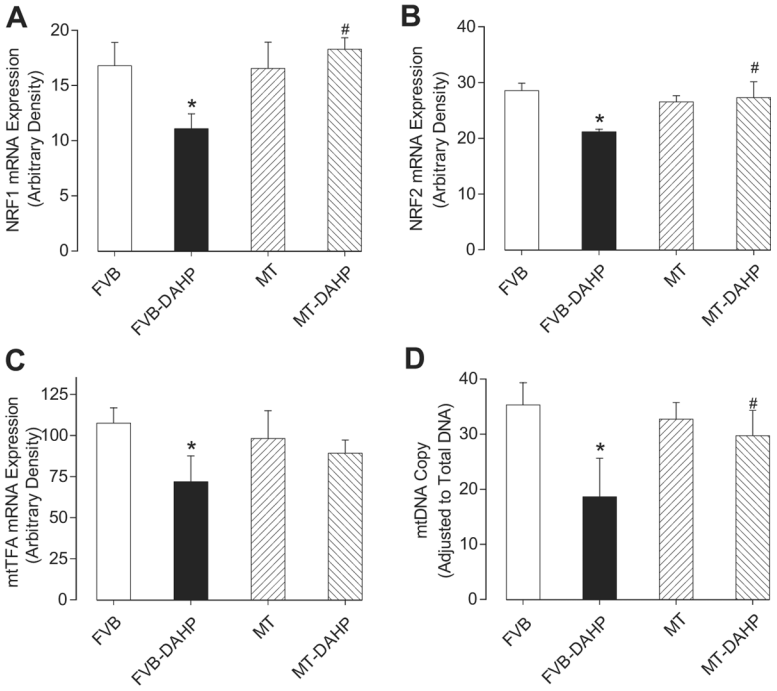

Fig. 6.

RT-PCR measurement of (A) nuclear respiratory factor 1 (NRF1), (B) nuclear respiratory factor 2 (NRF2), (C) mitochondrial transcription factor A (mtTFA) and (D) mtDNA copy number in left ventricles from FVB and MT mice with or without DAHP treatment. Mean ± SEM, n = 5–6, * $p<0.05$ *vs*. FVB, # $p<0.05$ *vs*. FVB-DAHP.

Table 1

General feature of FVB and MT mice with or without DAHP treatment for 3 weeks.

Parameter	FVB (34)	MT (34)	FVB-DAHP (32)	MT-DAHP (31)
Body Weight (g)	26.44 ± 0.42	27.48 ± 0.67	26.68 ± 0.45	27.56 ± 0.65
Heart Weight (HW, mg)	153 ± 7	156 ± 8	156 ± 8	148 ± 7
HW/Body Weight (mg/g)	5.77 ± 0.23	5.61 ± 0.20	5.89 ± 0.30	5.41 ± 0.21
Liver Weight (LW, g)	1.42 ± 0.05	1.40 ± 0.07	1.41 ± 0.05	1.38 ± 0.05
LW/Body Weight (mg/g)	53.7 ± 1.7	50.4 ± 1.6	53.1 ± 1.4	50.3 ± 1.4
Kidney Weight (KW, g)	0.341 ± 0.011	0.346 ± 0.014	0.360 ± 0.013	0.369 ± 0.014
KW/Body Weight (mg/g)	12.89 ± 0.30	12.45 ± 0.27	13.60 ± 0.41	13.34 ± 0.31
Systolic BP (mmHg)	103.3 ± 3.1	105.5 ± 3.2	145.8 ± 10.7*	140.5 ± 6.3*
Diastolic BP (mmHg)	72.5 ± 10.0	75.5 ± 5.5	117.0 ± 12.7*	101.8 ± 8.6*
Blood Glucose (mM)	5.10 ± 0.26	5.34 ± 0.27	5.41 ± 0.25	5.22 ± 0.30
Heart Rate (bpm)	545 ± 15	541 ± 20	557 ± 24	544 ± 19
Wall Thickness (mm)	0.871 ± 0.049	0.927 ± 0.063	0.712 ± 0.043*	0.868 ± 0.019†
EDD (mm)	2.32 ± 0.16	2.29 ± 0.21	2.04 ± 0.14	2.24 ± 0.16
ESD (mm)	1.15 ± 0.11	1.11 ± 0.12	1.42 ± 0.09*	1.23 ± 0.10†
LV Mass (mg)	66.9 ± 6.2	62.4 ± 9.2	53.6 ± 9.6	66.9 ± 8.5
Normalized LV Mass (mg/g)	2.35 ± 0.20	2.27 ± 0.30	1.92 ± 0.34	2.42 ± 0.28
Fractional Shortening (%)	50.6 ± 2.6	50.9 ± 4.1	36.7 ± 1.9*	45.3 ± 2.8†

Mean ± SEM,

number of mice per group is given in parentheses.

*p < 0.05 *vs.* FVB group,

†p < 0.05 *vs.* FVB-DAHP group,